Applied Biochemistry and Biotechnology (2022) 194:6319–6334
https://doi.org/10.1007/s12010-022-04027-y

ORIGINAL ARTICLE

Astragaloside IV in Hypoxic Pulmonary Hypertension: an *In Vivo* and *In Vitro* Experiments

XinTian[1] · Xiaofeng Zhang[2] · Yi Feng[3] · Xiaolong Gao[3] · Xuan Hao[3] · Junru Zhang[3] · Yunhong Long[3] · RongFang[3] · Shumiao Zhang[4] · Ling Li[5]

Accepted: 24 June 2022 / Published online: 2 August 2022

Abstract

The objective of study was to find the actions of astragaloside IV (ASIV) on PAH due to monocrotaline (MCT) in rats. Intraperitoneal injection of 60 mg/ kg MCT was injected to rats, come after by ASIV treatment with doses of 10 mg/kg daily once or 30 mg/kg of dose for twenty one days once daily. RVSP, serum inflammatory cytokines, RVH, and the other pathological parameters of the pulmonary arteries were evaluated. ASIV attenuated the increased pulmonary artery pressure and its structure in rat modification due to MCT. Additionally, ASIV avoided the rise in tumor necrosis factor (TNF)-α and interleukin (IL)-1β levels in the blood serum, and their expression of gene in the pleural parts, which was caused by MCT. ASIV promoted apoptotic resistance of HPASMCs and weakened the hypoxia-induced proliferation. ASIV shows over expression of caspase-3, caspase-9, p21, p27, and Bax, while ASIV downregulated Bcl-2, phospho-ERK, HIF-1α, and protein appearance in HPASMCs. These findings of the *in vitro* and the *in vivo* experiment indicate that astragaloside IV exerts protective effects against pulmonary arterial pressure, and may have action to be improved into pharmacological drug for pulmonary arterial pressure treatment.

Keywords Astragaloside IV · Inflammation · PAH · Pulmonary artery endothelial cells · Monocrotaline

✉ Ling Li
lilinghuxinxin@sina.com

[1] Department of Cardiology, Shaanxi Provincial Hospital of Chinese Medicine, No. 4 Xihuamen Street, Xian 710003, China

[2] Department of Nephrology, Shaanxi Provincial Hospital of Chinese Medicine, No. 4 Xihuamen Street, Xian 710003, China

[3] School of Graduate, Shaanxi University of Chinese Medicine, No.1 Middle Weiyang Road, Xianyang 712046, China

[4] School of Basic Medicine, Fourth Military Medical University, No. 169 Changle West Road, Xian 710032, China

[5] Department of Geriatrics, Shaanxi Provincial Hospital of Chinese Medicine, No. 4 Xihuamen Street, Xian 710003, China

Introduction

Monocrotaline (MCT) is a pyrrolizidine alkaloid which is formed from *Crotalaria spectabilis*, which is hepatotoxic and pneumotoxic in the animals, for example, rat. The MCT single injection can cause progressive pulmonary hypertension may result in the right ventricular hypertrophy and cardiac failure [1–3]. Pathological changes and hemodynamic changes related with MCT administration include degeneration and fragmentation of endothelial cells, edema of perivascular tissues, blebbing of the lung [4–9], muscularization of the pulmonary arterioles and arteries, and extravasation of red blood cells [10–16]. Rats report ascites and pleural effusions with severe right ventricular hypertrophy due to MCT [17, 18].

Astragalus membranaceus is an herb utilized in People's Republic of China to treat various kinds of diseases from long ago, for example, cardiovascular diseases, kidney diseases, allergic rhinitis, hepatitis, and skin diseases [19, 20]. Astragaloside IV (ASIV) is the predominant bioactive compound obtained from the *Astragalus membranaceus* [21]. ASIV is a natural triterpenoid glycoside [22]. In the myocardium, lack of a blood and/or oxygen supply could lead to weaken cardiac function and compromise health. ASIV could protect the myocardial cells of rats due to the low oxygen supply results in the cytoplasm of the myocardium cells raised content and activity of super-oxide dismutase (SOD) [23]. Study indicated that ASIV has diverse pharmacologic actions like immunomodulatory, anti-inflammatory, antiviral, and anti-apoptosis [24]. Also, data have shown that ASIV has a defensive effect on pulmonary hypertension [25]. In an ovalbumin-evoked asthma model, ASIV alleviates airway inflammation and airway hyperresponsiveness [26]. Besides, in the chronic hypoxia-induced pulmonary hypertension model, ASIV improves pulmonary function through suppression of the tumor necrosis factor (TNF)-α and secretion of interleukin (IL)-6 [27].

PAH has a complicated aetiology that is not totally understood. The imbalance between pulmonary artery smooth muscle cell (PASMC) proliferation and death causes pulmonary vascular remodeling, which is an essential sign of the severity and development of PAH [26–29].

Astragalus membranaceus, which has been regarded as a commonly utilized plant in China, yields astragaloside IV (ASIV), a high-purity medication. Numerous pharmacological actions are produced by ASIV, including anti-oxidative, anti-inflammatory, cardioprotective, and anti-cancer properties. ASIV has been shown in prior studies to be protective against the pulmonary fibrosis and acute lung damage caused by sepsis and bleomycin, respectively, in rats. These results also suggested that ASIV may be protective against lung disorders [20–28].

Pulmonary arterial hypertension (PAH) is a cardiovascular condition with higher mortality and morbidity [28]. PAH is a rare, growing disorder with characters like hypertension of pulmonary artery for no apparent reasoning. Pulmonary hypertension is considered if average pulmonary artery pressure is 25 mm Hg or high in a resting condition. The pulmonary arteries are type of the blood vessels that bring blood to the lungs from the right ventricle of the heart. The symptoms of this include pain in the chest, fainting episodes, and shortness of breath (dyspnea) especially during exercise. The first time PAH occurred in 1891, where at autopsy indicated thickening of the pulmonary artery published by a German doctor E. Romberg. The abnormal bluish discolored skin may have seen in advanced stages of PAH due to decreased levels of circulating blood oxygen (cyanosis). Also, in extreme cases, abnormal enlargement of the right ventricle of the heart (hypertrophy) leads

to the declined function of the right chamber of the heart and, likely, failure of the right portion of heart. About 15–20% of cases who had PAH may have inheritable PAH. It is an autosomal dominant genetic disorder because of changes in the most commonly BMPR2 gene, though other genes (mutations)[29].

Materials and Methods

Ethics Approval

The experiment was approved by the animal ethics committee of the institute (Protocol number 15BvCG).

Chemicals, Reagents, and Antibodies

ASIV was obtained from Santa Cruz Biotechnology, Dallas, TX, USA. Angiotensin II, TNF-α IL-6 and Endothelin-1. ELISA kits were purchased from Abcam Inc., Cambridge, UK. The CCK8 kit (Cell Counting Kit-8) was purchased from Kumamoto, Mashikimachi, Japan. Acetonitrile (HPLC grade) and methanol were purchased from Thermo Fisher Scientific, Inc., Waltham, MA, USA. From the Guoan Institute of Biotechnology, Shanghai, China, sodium pentobarbital was purchased.

Preparation of Monocrotaline Solution

In 1 N HCl, MCT was dissolved and dilution was done by normal saline. The pH of this solution was d to 7.4.

Preparation of Astragaloside IV

ASIV was initially dissolved in 0.5% DMSO, diluted in a normal saline.

Animals

Eight weeks old and weighing 200–230 g male animals were used in the study. The rats were housed at a controlled environment with 12-h light/dark cycles. Food and water were provided.

Allocation of Treatment

The rats were split up into 4 categories (6 in each category) as follows: (1) the control group; (2) the MCT group; (3) the MCT + ASIV (10 mg/kg/day) group; and (4) the MCT + AS IV (30 mg/kg/day) group. The intraperitoneal injection of 60 mg/kg MCT was administered to induce PAH in group 2 to 4. The rats in the control group were given the equal volume of 0.5% DMSO.

There were symptoms of damage in pulmonary vascular endothelial after 1 h of the intraperitoneal MCT injection, but pulmonary artery pressure was not increased. Then,

in the next 2 weeks, pressure of pulmonary artery starts to rise. On following for 48 h of the MCT administration, ASIV were given intraperitoneally once daily for next 21 days.

Hemodynamic Parameter

After hypoxia, rats with intraperitoneal injection of 250 mg/kg tribromoethanol were anesthetized, and through the right jugular vein, a polyethylene (PE) catheter was inserted into the right ventricle (RV) and right ventricular systolic pressure (RVSP) was recorded. Then, septum (S), left ventricle (LV), and RV were isolated, and LV and RV + S were weighed. The ratio of RV/(LV + S) (Fulton index) was evaluated and used as an index for right ventricular hypertrophy.

Structural Parameters

3-mm-slices from lungs were cut and immersed in 4% w/v neutral-buffered formalin. The paraffin embedding was done on the sliced lung pieces and dissected into 4 μm thickness. Then, dewaxing was performed in xylene for that lung portions, saturated with graded ethanol and staining was done by eosin and hematoxylin. To evaluate pulmonary artery structural remodeling, the percentage medial wall thickness (% WT) and percentage medial wall area (% WA) were derived per Eq. 1 and Eq. 2:

$$\% \text{ Wall thickness} = \frac{\text{Outside dia} - \text{inside dia}}{\text{Outside dia}} \times 100 \tag{1}$$

$$\% \text{ area of medial wall} = \frac{\text{Area of Medial wall}}{\text{Area of Total vessel}} \times 100 \tag{2}$$

Staining of Immunohistochemical

The dewaxing of lung slices was done in xylene and saturated with graded ethanol, and antigens were recovered. With the help of 5% bovine serum albumin, unspecific protein binding was blocked by treating for half an hour at normal temp. The anti-PCNA antibody (1:1000) or anti-α-SMA antibody (1:500) was used for overnight incubation at 4 °C temperature. Then, a biotinylated anti-mouse immunoglobulin G antibody is used for incubation for 1 h. Hematoxylin was used for counterstaining for 5 min. The evaluation of PCNA and α-SMA antibodies was done.

Cell Viability Assay For 24 h, cell cycle arrest was applied to PASMCs. Cells were then moved to PBS with 5% FBS and incubated for 48 h at room temperature in normoxic or hypoxic conditions. A 48-h AS-IV treatment in hypoxic settings was administered to cells after a 1-h DAPT pretreatment. After that, PASMCs were grown for 4 h at 25 °C in media containing 0.5% MTT. The purple formazan was dissolved in DMSO for 10 min at 37℃. Using a spectrophotometer, the absorbance was determined at a wavelength of 540 nm.

Role of RTQPCR

TRIzol chemical was used for extraction of Total RNA from samples (Waltham, MA, USA). Applied Light Cycler 2 System (Germany) and SYBR-Green I reagent (Shiga, Japan) were used for the analysis of RT-qPCR. The relative expression levels of tumor necrosis factor-alpha and interleukin-1 *beta* were determined where internal control was β-actin.

Measurement of Pulmonary Arterial Pressure Rats were weighed and anaesthetized with an intraperitoneal dose of 40 mg/kg sodium pentobarbital after 6 weeks of hypoxia exposure. A micro-catheter (0.9 mm inner diameter) was progressively introduced into the pulmonary artery via the right external jugular vein. A BL-420F biological and functional information collecting system was used to collect and evaluate mean pulmonary arterial blood pressure (mPAP) after a 30-min equilibration time (Biolap 420F; Chengdu TaiMeng Technology Co.).

Hypoxia and Cell Culture

Primary human PAECs and human PASMCs were obtained from Sciencell Research Laboratories Inc., Carlsbad, CA, USA. The HPAECs were cultured in ECM (5% phosphate buffer solution, 1% ECGS), HPASMCs were cultured in DMEM supplemented with 10% phosphate buffer solution, and the cells used in the experiments were between passages 3 and 8. These cells were categorized into six groups as follows: the normoxia, hypoxia, hypoxia + 10 μM ASIV, hypoxia + 20 μM ASIV, hypoxia + 40 μM ASIV, and hypoxia + 80 μM ASIV groups, and then cultured either under normoxic or hypoxic conditions for 24 h.

Assessment of HPASMC

The multiplication of HPASMCs was evaluated by MTT (3-(4,5-dimethylthiazol-2-yl)-2,5-diphenyl tetrazolium bromide) assay. The HPASMCs were cultured under normoxic or hypoxic condition 96-well plates (5000 cells per well), and then, in the following treatment, a 5 mg/ml concentrated MTT solution was added to each well, and the plates were incubated at 37 °C for 4 h. Finally, DMSO was added. The optical density (OD) of the samples was measured at 570 nm in a microplate spectrophotometer (BioTek Instruments, Inc., Winooski, VT, USA).

Apoptosis Evaluation

TUNEL staining was used for the evaluation of HPASMC apoptosis. The incubation of lung tissue is performed by 3% water for 10 min, but first they were dewaxed in xylene and dehydrated with HPLC-graded ethanol and proteinase K was used for further incubation for 30 min and then go for TUNEL reaction in the dark for 1 h at 37℃. The brown color apoptotic cells were observed with diaminobenzidine and counterstained with hematoxylin for 5 min. HPASMCs were fixed in 4% paraformaldehyde for 30 min.

Table 1 Hemodynamic and morphological parameters and OD value of α-SMA

Group	RVSP (mmHg)	Fulton index	% Medial wall area	% Medial wall thickness	Optical density value of α-SMA
Control	18.97 ± 0.2830	0.235 ± 0.0056	39.83 ± 0.6009	25.5 ± 0.5627	402.67 ± 5.566
MCT	43.26 ± 0.4726	0.442 ± 0.0079	79 ± 0.7746	55.5 ± 0.7638	799.5 ± 6.850
ASIV10	37.59 ± 0.5143	0.357 ± 0.0042	62.83 ± 0.6009	37.83 ± 0.6009	600 ± 10.076
ASIV30	28.09 ± 0.7661	0.245 ± 0.0076	57.67 ± 0.4944	33.67 ± 0.4216	539.83 ± 4.269

RVSP, right ventricular systolic pressure. Values are depicted in means ± standard error of mean (SEM)

Table 2 Results of assays

Group	PCNA positive cells	TUNEL positive cells	Serum TNF-α level (pg/ml)	Serum IL-1β level (pg/ml)
Control	19.33 ± 0.4944	17.33 ± 0.4216	31.5 ± 0.4282	135.16 ± 1.537
MCT	54.17 ± 0.9804	12.5 ± 0.4282	54 ± 0.5164	311.17 ± 1.493
ASIV 10	36 ± 0.5774	22.66 ± 0.4944	42.83 ± 0.6009	207.83 ± 1.869
ASIV 30	33.33 ± 0.4944	25.66 ± 0.4216	37 ± 0.5774	198.83 ± 0.6009

TUNEL, the terminal deoxyribonucleotidyl transferase-mediated dUTP nick end-labeling

Subsequently, the cells were treated with Triton X-100 for 5 min and then incubated with TUNEL reaction mixture for 60 min at 37 °C in the dark area.

Localized green fluorescence of apoptotic FITC-labeled TUNEL-positive cells was imaged using a fluorescence microscope (Carl Zeiss AG, Jena, Germany), and images of 4 random and non-overlapping fields were selected from each well of 12-well plates at × 400 magnification for analysis purposes. The sections were then incubated with proteinase K than TUNEL reaction at 37℃ for 30 min.

Assay of Tumor Necrosis Factors Alpha and Interleukin 1-Beta

For serum collection, blood sample were centrifuged at 1500 rpm for 20 min at 4℃. HPAEC culture media was used. ELISA kits were used for measurement of the concentration of tumor necrosis factors alpha and interleukin 1-beta.

Statistical Data

GraphPad Prism 7.05 was used for all statistical calculations, and all results are provided as the mean SD (GraphPad Software, Inc.). One-way analysis of variance (ANOVA) and Tukey's post hoc test were used to examine group differences. A statistically significant difference was determined if P value was less than 0.05.

Results

Hemodynamic and Morphological Parameters, OD Value of α-SMA

The results of hemodynamic and morphological parameters and OD value of α-SMA are reported in Tables 1 and 2.

The formation of PAH is shown by the RVSP value of MCT being greater than the control group. However, this pathophysiological shift was averted with therapy using both dosages of ASIV 10 and ASIV 30. PAH and RV hypertrophy were reduced with ASIV. Figure 1 displays the RVSP values for the various groups. In comparison to the controls, the

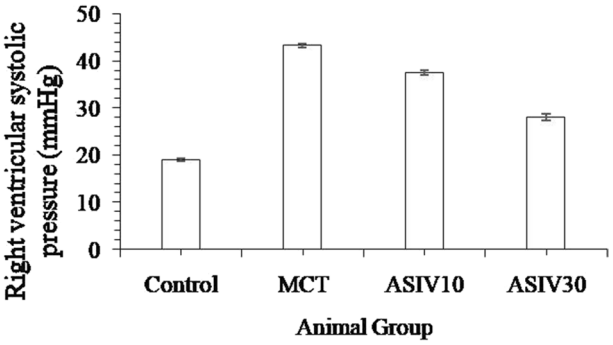

Fig. 1 Right ventricular systolic pressure values in various groups of rats. Six rats in each group

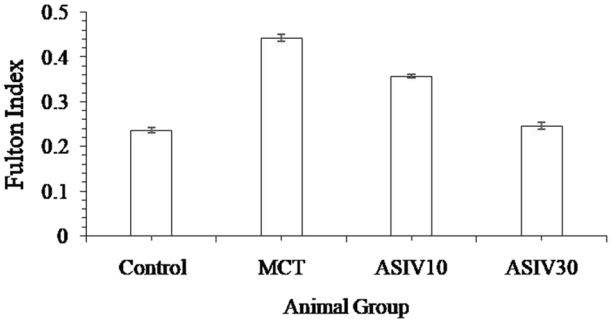

Fig. 2 Fulton index values in various groups of rats

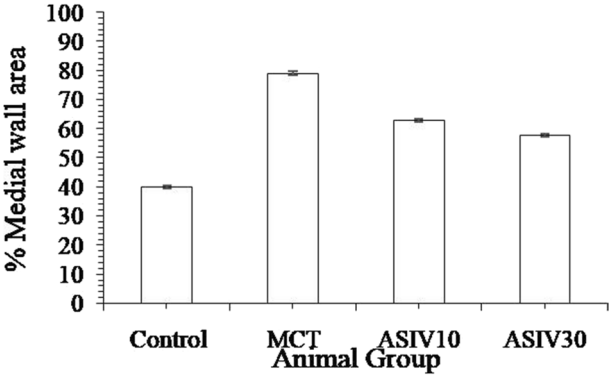

Fig. 3 % area of Medial wall in various groups of rats

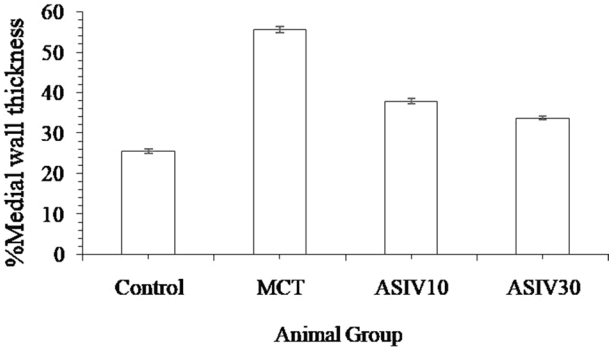

Fig. 4 % thickness of Medial wall of pulmonary arteries in various groups of rats

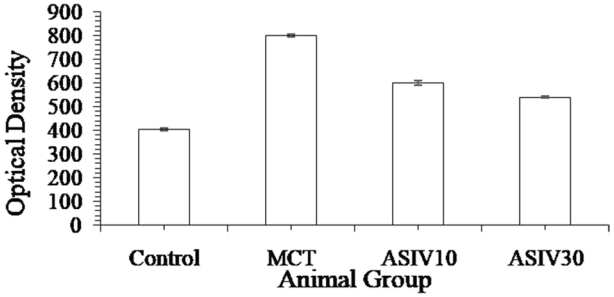

Fig. 5 Quantitative estimation of the optical density value of α-SMA immunoreactivity in pulmonary arteries in various groups of rats

Fulton index increased in the MCT group. Figure 2 displays the Fulton index values for the various groupings. The MCT significantly increased the percentage of WA and WT pulmonary arteries, as seen in Figs. 3 and 4; however, treatment with 10 and 30 mg/kg/day ASIV attenuated these pathological alterations, demonstrating the development of pulmonary artery structural remodeling. The α-SMA levels showed the hyperplastic smooth muscularization arteries. However, ASIV attenuated α-SMA expression in pulmonary arteries (Fig. 5).

PASMC Multiplication

Expression of PCNA was measured in the medial side of pulmonary arteries for evaluation of the role of ASIV in PASMC proliferation. The numbers of PCNA-positive cells as compared to the smooth muscle cells in the rats of the MCT group were highly more than the rats of control group with significant p value of less than 0.05. Although, treatment with doses of ASIV decreased the uncommon multiplication of PASMC. MTT assay revealed that ASIV reticent the hypoxia-induced HPASMC proliferation,and the effects were concentration-dependent (i.e., AS IV 30 group had higher effect than that of AS IV 10 with significant p value. ASIV reduces expression of PCNA (Fig. 6).

Under normoxic or hypoxic conditions, the proliferation of HPASMC was recorded after treating with different ASIV concentrations. In the HPASMCs induced by hypoxia, the results of blot analysis found that ASIV everted the HIF-1α enhancement (Fig. 7) and p-ERK1/2protein expression (Fig. 8), and also reduces in p21 and p27 levels with significant p values. ASIV inhibits hypoxia-induced HPASMC proliferation.

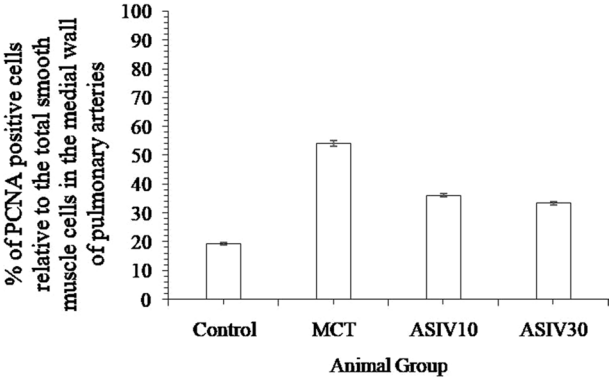

Fig. 6 comparison of % of PCNA-positive cells and smooth muscle cells

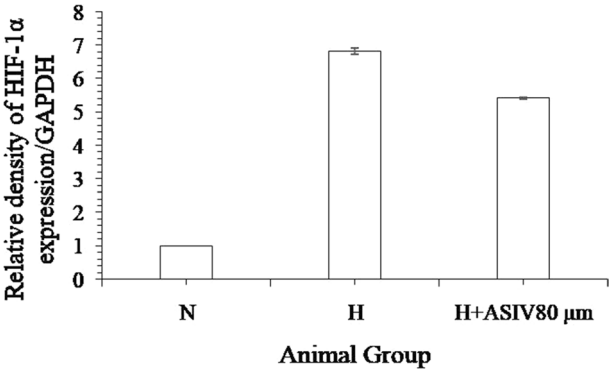

Fig. 7 Western blot analysis for HIF-1α level. N, normoxia; H, hypoxia

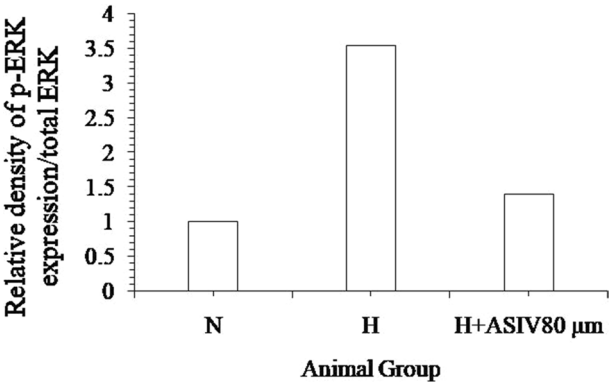

Fig. 8 Western blot analysis for p-ERK1/2 protein levels

Apoptosis of PASMC

A TUNEL assay was done to evaluate effects of apoptotic resistance of PASMCs by ASIV. Figure 9 explained the disturbed apoptosis that was seen, whereas ASIV concentrations significantly raised apoptosis of PASMC. The green fluorescence of the free labeled 3′-OH termini was to show apoptotic HPASMCs *in vitro*. This concluded

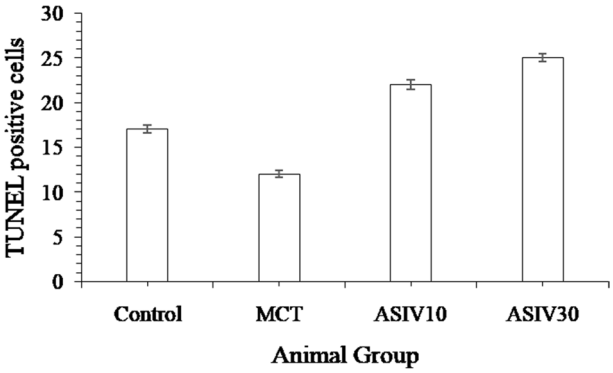

Fig. 9 TUNEL assay comparison of number of TUNEL-positive cells with total smooth muscle cells

that rather under normoxic conditions, the apoptotic cells percentage under hypoxic conditions was significantly reduced, while hypoxia-induced apoptotic resistance was reversed by ASIV.

The levels of apoptosis-related proteins in the HPASMCs were detected by western blot analysis. Hypoxia markedly decreased the levels of the pro-apoptotic proteins, Bax, cleaved caspase-9, and cleaved caspase-3, while it increased the expression of the anti-apoptotic protein, Bcl-2, in HPASMCs. However, ASIV treatment normalized these alterations. ASIV promotes HPASMC apoptosis (Figs. 10 and 11).

Anti-inflammatory Effects and RT-qPCR Analysis

Serum levels of tumor necrosis factor and interleukin-1 were assessed for ASIV's anti-inflammatory effects. Figures 12 and 13 indicated that levels increased in the MCT group, but increases were prevented by ASIV at both dosages. The RT-qPCR analysis revealed that the MCT group had higher levels of lung tissue TNF-alpha and interleukin-1 mRNA expression than the control group, which was likewise normalized by both dosages of ASIV. The elevated expression of both in pleural tissues and serum was diminished by ASIV.

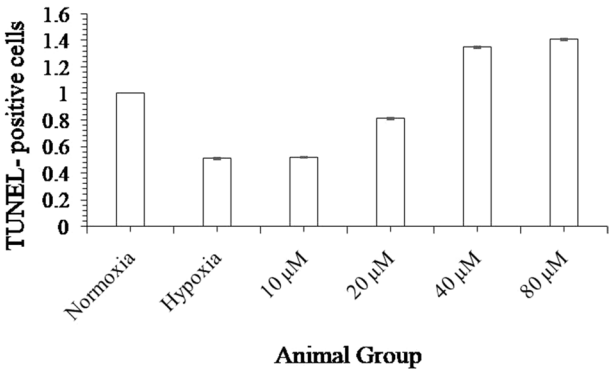

Fig. 10 Western blot analysis for TUNEL cells

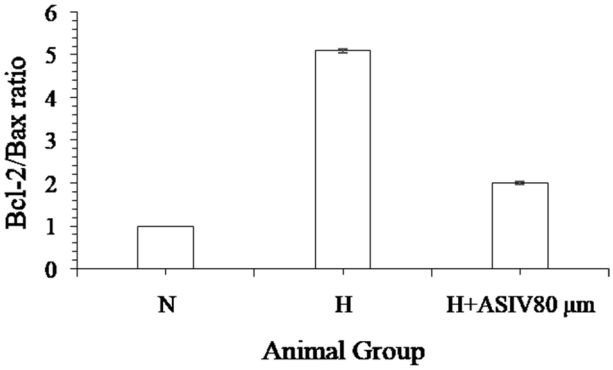

Fig. 11 Western blot analysis forBcl-2

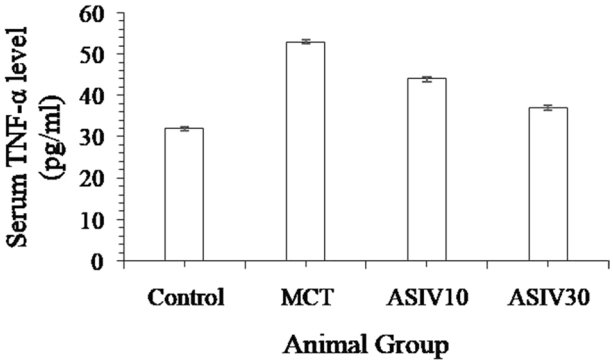

Fig. 12 Serum TNF-α level estimation

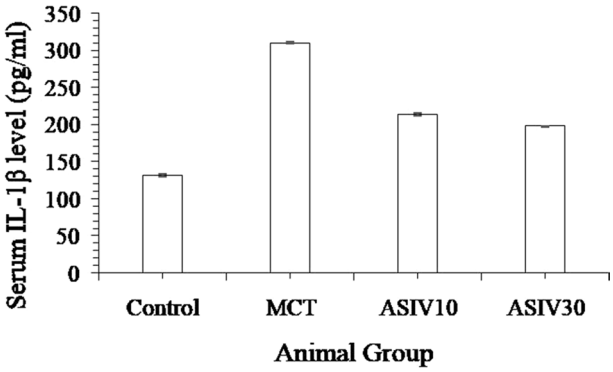

Fig. 13 Serum IL-1βanalysis

Dysfunctioning of HPAEC

TNF- and interleukin-1 levels are higher in hypoxia (Figs. 14, 15, 16 and 17) than in normoxia (Fig. 16) in the supernatants of the HPAEC culture medium. ASIV treatment, however, prevented those changes in levels. Furthermore, HPAECs' HIF-1 and VEGF protein levels were elevated by hypoxia, which were reduced by ASIV therapy, according to western blot analysis.

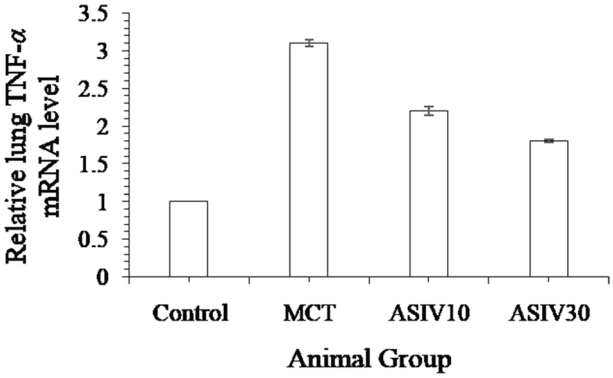

Fig. 14 RT-qPCR analysis of TNF-α in rat lung tissues

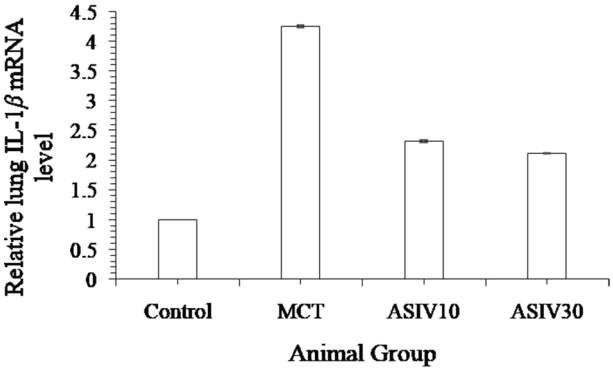

Fig. 15 RT-qPCR analysis of IL-1βin rat lung tissues

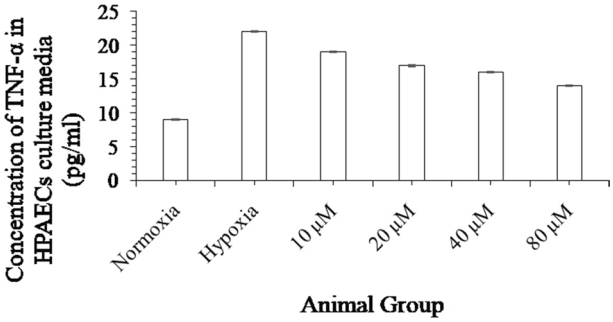

Fig. 16 TNF-α concentration in HPAEC culture media

Discussion

In our current study, the MCT group rats have significantly raised pulmonary artery pressure, right ventricular hypertrophy, and pulmonary artery remodeling. But, these pathophysiological characteristic differences were overcome with doses (10 mg/kg/day and 30 mg/kg/day) of ASIV. Moreover, it reduced the elevation of tumor necrosis factor-α and interleukin-1 *beta* secretion in the serum and their gene expression in the pleural tissues, which were induced by MCT. Additionally, ASIV normalized the abnormal proliferation

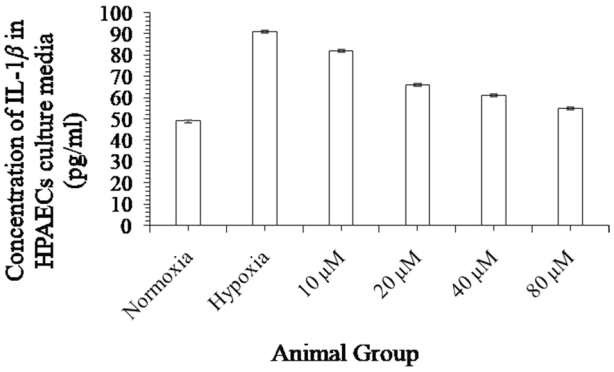

Fig. 17 IL-1β concentration in HPAEC culture media

and resistance of apoptosis for PASMCs and PAEC dysfunction in *in vitro* as well as the *in vivo* experiments. The results show that both doses of ASIV exert protective effects in PAH induced by MCT in rats. Pulmonary function tests might allow accurate and reproducible assessment of the functional conditions of the respiratory system. However, it could be interesting to find if ASIV can provide protective effects on respiratory systems or not. Protective effects of ASIV on the respiratory system require further investigation.

The persistent inflammation was disease-induced parameters in the MCT-induced PAH. In the pleural tissues, there can be elevation in inflammatory cytokines expression and inflammatory cells by one dose of MCT. Tumor necrosis factor-α and interleukin-1 *beta* are attached with the accumulation of extra cellular matrix proteins in PAH lesions and poor clinical outcomes in patients with PAH. Furthermore, serum levels of TNF-α and IL-1β are higher in patients with PAH than in normal patients, and serve as biomarkers of diseased conditions (PAH) [27]. TNF-α elevates pulmonary arterial reactivity and inhibits the vasodilating action of prostacyclin through the downregulation of prostacyclin synthase mRNA expression [28]. Furthermore, the overexpression of TNF-α in alveolar type-II cells causes an increase in the lung volume, alveolar enlargement, and an increase in the pulmonary artery pressure [29]. However, blocking of TNF-α and IL-1β signaling lead to ameliorate pulmonary inflammation, pulmonary hemodynamics, pulmonary vascular remodeling, and right ventricular hypertrophy [30–32]. ASIV attenuates some inflammation associated with cardiopulmonary diseases, such as obesity-related hypertension and cigarette smoke-induced pulmonary inflammation by decreasing the levels of TNF-α and IL-1β [33, 34]. In our study, ASIV defeats the inflammation reaction in rat of PAH. PASMCs in patients with PAH show large expansion and apoptosis-resistant behavior like some cancer cells, those related for increased pulmonary arterial pressure. It is an important parameter for the treatment of PAH. Our result shows that immune-histochemical analysis with a TUNEL and anti-PCNA antibody assay reported that ASIV defeat the expansion and apoptosis of PASMCs. HIF-1α, as an oxygen-sensitive transcription factor, is involved in the crosstalk among several hypoxia-related signaling pathways and promotes pulmonary artery structural remodeling by increasing proliferation and suppressing apoptosis [35]. Pulmonary hypertension was caused by changes in pulmonary artery through suppression of the PASMC [36]. For growth survival and proliferation, MAPK/ERK and PI3K/Akt signaling pathways play an important role [37]. We found in the *in vitro* experiments that HPASMCs was beneficial for detection of protein expression. Side by side, p-ERK1/2 and p-Akt protein

expression was detected. ASIV reversed the enhancement ofp-ERK1/2protein expression in HPASMCs induced by hypoxia, but not p-Akt protein expression. p27 and p21 are cyclin-dependent kinase inhibitors which have an important role in the regulation of cell cycle progression. Current data [38] have reported that they show inhibitory outcome on PASMC multiplication. The suppression of boost signaling, such as ERK1/2 can inhibit the degradation of p27 and p21 [39]. The results of the current study demonstrated that ASIV upregulated the protein expression of p21 and p27 in HPASMCs. Bcl-2 family proteins is participate for cell death. For higher and lower apoptotic thresholds, Bcl-2/Bax protein ratio is very significant in mitochondria apoptotic pathway.

In the present study, to determine whether ASIV-induced PASMC apoptosis is associated with the Bax/Bcl-2 and mitochondrial apoptosis pathways, the protein expression of Bcl-2, Bax, cleaved caspase-9, and cleaved caspase-3 was evaluated in HPASMCs. The results of the current study found that ASIV upregulated the protein expression of Bax, cleavedcaspase-9, and cleaved caspase-3 in HPASMCs, but downregulated Bcl-2proteinexpression. Collectively, these findings reported that ASIV can reduce PASMC proliferation and apoptotic resistance.

In the pulmonary vasculature structure, PAECs are found as the innermost part of the blood vessel and they work as the main barrier. In PAH, the affliction of PAECs leads to the disability of endothelial-dependent vasodilatation, a decrease in anticoagulant properties, elevated levels of adhesion molecules, an enhancement to reactive oxygen species production, and the release of different inflammatory cytokines [40]. In addition, the dysfunction of PAECs results to the increased angiogenesis that results plexiform lesion formation [38]. In the present study, it was observed that ASIV significantly reduced the increased HIF-1a and VEGF protein levels in HPAECs induced by hypoxia.

Conclusions

The present *in vitro* and the *in vivo* experiments demonstrated that the administration of Astragaloside IV better the pathological changes in pulmonary artery structural remodeling, and pulmonary arterial pressure, in a rat model of pulmonary arterial hypertension due to monocrotaline. The improvement of the inflammatory response, pulmonary artery endothelial cells dysfunction, and abnormal pulmonary artery cell proliferation and apoptotic resistance decreased in concentration-dependent manner with therapeutics response of astragaloside IV. These findings of the *in vitro* and the *in vivo* experiment indicate that astragaloside IV exerts protective effects against pulmonary arterial pressure, and may have action to be improved into pharmacological drug for pulmonary arterial pressure treatment. The significance of the research is that ASIV might display important therapeutic functions for the prevention and treatment of cardiovascular disorders, such as PAH. The precise molecular mechanisms of action of astragaloside IV for pulmonary arterial pressure require further investigation.

Author Contribution All authors contributed equally.

Data Availability Not applicable.

Declarations

Ethical Approval The experiment was approved by the animal ethics committee of the institute (Protocol number 15BvCG).

Consent to Participate All authors have their consent to participate.

Consent to Publish All authors have their consent to publish their work.

Competing Interests The authors declare no competing interests.

References

1. Gillespie, M. N., Goldblum, S. E., Cohen, D. A., & McClain, C. J. (1988). Interleukin-1 bioactivity in the lungs of rats with monocrotaline-induced pulmonary hypertension. *Proceedings of the Society for Experimental Biology and Medicine, 187*, 26–32.
2. Gillespie, M. N., Olson, J. W., Reinsel, C. N., & O'Connor, W. N. (1986). Altiere and RJ, Vascular hyperresponsiveness in perfused lungs from monocrotaline-treated rats. *The American Journal of Physiology, 251*, H109–H114.
3. Todorovich-Hunter, L. J. D., Ranger, P., & Keeley, F. W. (1988). Rabinovitch and M, Altered elastin and collagen synthesis associated with progressive pulmonary hypertension induced by monocrotaline. A biochemical and ultrastructural study. *Laboratory Investigation, 58*, 184–195.
4. Hislop, A. R. L. (1979). Arterial changes in Crotalaria spectabilis-induced pulmonary hypertension in rats. *British Journal of Experimental Pathology, 55*, 153–163.
5. Huxtable, R. D. C. D., & Eisenstein, D. (1978). The effect of a pyrrolizidine alkaloid, monocrotaline, and a pyrrole, dehydroretronecine, on the biochemical functions of the pulmonary endothelium. *Molecular Pharmacology, 14*, 1189–1203.
6. Lalich, J. J. J. W., Raczniak, J. J., & Shumaker, R. C. (1977). Fibrin thrombosis in monocrotaline pyrrole induced cor pulmonale in rats. *Archives of Pathology & Laboratory Medicine, 101*, 69–73.
7. Meyrick, B. G. W., & Reid, L. (1980). Development of Crotonolaria pulmonary hypertension: A hemodynamic and structural study. *American Journal of Physiology, 239*, H692–H702.
8. Meyrick, B. R. L. (1979). Development of pulmonary arterial changes in rats fed Crotalaria spectabilis. *American Journal of Physiology, 94*, 37–50.
9. Valdiva, E. L. J., Hayashi, Y., & Sonnard, J. (1967). Alterations in pulmonary alveoli after a single injection of monocrotaline. *Archives of Pathology, 84*, 64–76.
10. Altiere, R. J. M. M., Petrenka, J., Olson, J. W., & Gillespie, M. N. (1986). Altered pulmonary vascular smooth muscle responsiveness in monocrotaline-induced pulmonary hypertension. *J Pharmacology and Experimental Therapeutics, 236*, 390–395.
11 Ghodsi, F. W. J. (1981). Changes in pulmonary structure and function induced by monocrotaline intoxication. *American Journal of Physiology, 240*, H149–H155.
12 Hilliker, K. S. B. T., & Roth, R. A. (1982). Pneumotoxicity and thrombocytopenia after single injection of monocrotaline. *American Journal of Physiology, 242*, H573–H579.
13. Hilliker, K. S. R. R. (1985). Increased vascular responsiveness in lungs of rats with pulmonary hypertension induced by monocrotaline pyrrole. *American Review of Respiratory Diseases, 131*, 46–50.
14 Lai, Y. L. T. A. (1996). Diana JN Hypoxemia and elevated tachykinins in rat monocrotaline pneumotoxicity. *Lung, 174*, 195–203.
15 Molteni, A. W. W., TsAo, C. H., Solliday, N. H., & Dunne, M. (1985). Monocrotaline-induced pulmonary fibrosis in rats: Amelioration by captopril and penicillamine. *Proceedings of the Society for Experimental Biology and Medicine, 180*, 112–120.
16. Stenmark, K. R. M. M., Remigo, L. K., Voelkel, N. F., Murphy, H. P. R. C., Mathias, M. M., & Reeves, J. T. (1985). Alveolar inflammation and arachidonate metabolism in monocrotaline-induced pulmonary hypertension. *American Journal of Physiology, 248*, 859–866.
17 Ceconi, C. C. E., Quinzanini, M., Rodella, A., Ferrari, R., & Noradrenaline, H. P. (1989). atrial natriuretic peptide, bombesin and neurotensin in myocardium and blood of rats in congestive cardiac failure. *Cardiovascular Research, 23*, 674–682.
18. Vogel HG, Drug discovery and evaluation: Pharmacological assays. 3 ed. 2007: Springer.

19. Guo, H. L. M. (2013). Mechanism of traditional Chinese medicine in the treatment of allergic rhinitis. *Chinese Medical Journal (Engl), 126*(4), 756–760.
20 Ren, S. Z. H., & Mu, Y. (2013). Pharmacological effects of Astragaloside IV: A literature review. *Journal of Traditional Chinese Medicine, 33*(3), 413–416.
21 Li, L. H. X., & Xu, R. (2017). Research review on the pharmacological effects of astragaloside IV. *Fundamental & Clinical Pharmacology, 31*(1), 17–36.
22. Yaochen, C. L. Z., & Wang, Y. U. (2019). Astragaloside IV attenuates renal fibrosis through repressing epithelial-to-mesenchymal transition by inhibiting microRNA-192 expression: And studies. *The American Journal of Translational Research, 11*, 5029–5038.
23 Ren, S. (2013). Pharmacological effects of Astragaloside IV A literature review. *Journal of Traditional Chinese Medicine, 33*(3), 413–416.
24 Zhang, J. W. C., & Gao, L. (2020). Astragaloside IV derived from Astragalus membranaceus: A research review on the pharmacological effects. *Advances in Pharmacological, 87*, 89–120.
25. Shumin, Q. J. Y., & Shaogang, H. (2019). Astragaloside IV protects ethanol-induced gastric mucosal injury by preventing mitochondrial oxidative stress and the activation of mitochondrial pathway apoptosis in rats. *Frontiers in Pharmacology, 10*, 894.
26. Yang, X. W. F. (2019). The effect of astragaloside IV on JAK2-STAT6 signalling pathway in mouse model of ovalbumin-induced asthma. *Journal of Animal Physiology and Animal Nutrition (Berl), 103*(5), 1578–1584.
27 Zhang, X. C. J., & Xu, P. (2018). Protective effects of astragaloside IV against hypoxic pulmonary hypertension. *Medicinal Chemistry Communications, 9*(10), 1715–1721.
28 Simonneau, G. M. D., & Celermajer, D. S. (2019). Haemodynamic definitions and updated clinical classification of pulmonary hypertension. *European Respiratory Journal, 53*(1), 1801913.
29. Fox, K. Pulmonary Arterial Hypertension. 2022 [cited 2022 16 January]; Available from: https://rareiseases.org/rare-diseases/pulmonary-arterial-hypertension/.
30. Groth, A. V. B., Brock, M., Speich, R., Ulrich, S., & Huber, L. C. (2014). Inflammatory cytokines in pulmonary hypertension. *Respiratory Research, 15*, 47.
31 Wang, Q. Z. X., Wang, Y. Y., Xie, W. P., Wang, H., & Zhang, M. (2013). Monocrotaline-induced pulmonary arterial hypertension is attenuated by TNF-α antagonists via the suppression of TNF-α expression and NF-κB pathway in rats. *Vascular Pharmacology, 58*, 71–77.
32. E CMaS, Pulmonary arterial hypertension in adult-onset still's disease: Rapid response to anakinra. Case Reports in Rheumatology, 2012: 537613
33. Jiang, P. M. D., Wang, X., Wang, Y., Bi, Y., Yang, J., Wang, X., & Li, X. (2018). Astragaloside IV prevents obesity-associated hypertension by improving pro-inflammatory reaction and leptin resistance. *Molecules and Cells, 41*, 244–255.
34 Meiqian, Z. L. Z., & Chang, C. (2018). Astragaloside IV inhibits cigarette smoke-induced pulmonary inflammation in mice. *Inflammation, 41*, 1671–1680.
35. ED, P. R. A. M. (2014). The metabolic theory of pulmonary arterial hypertension. *Circulation Research, 115*, 148–164.
36. Ball, M. K. W. G., Mungai, P. T., Nielsen, J. M., Czech, L., Dudley, V. J., Beussink, L., Dettman, R. W., Berkelhamer, S. K., & Steinhorn, R. H. (2014). Regulation of hypoxia-induced pulmonary hypertension by vascular smooth muscle hypoxia-inducible factor-1α. *American Journal of Respiratory and Critical Care Medicine, 189*, 314–324.
37. Wang, G. W. J., Fu, X. L., Guang, R., & To, S. T. (2017). Advances in the targeting of HIF-1α and future therapeutic strategies for glioblastoma multiforme (Review). *Oncology Reports, 37*, 657–60.
38. Jin, H. J. Y., Guo, L., Ma, Y., Zhao, R., Li, X., Shen, L., Zhou, Z., Kim, S. C., & Liu, J. (2021). Astragaloside IV blocks monocrotaline-induced pulmonary arterial hypertension by improving inflammation and pulmonary artery remodeling. *International Journal of Molecular Medicine, 47*(2), 595–606.
39. Ashok, C. O. S., Srijyothi, L., Selvam, M., Ponne, S., & Baluchamy, S. (2019). A feedback regulation of CREB activation through the CUL4A and ERK signaling. *Medical Oncology, 36*, 20.
40. Humbert, M. G. C., Bonnet, S., Dorfmüller, P., Klinger, J. R., Nicolls, M. R., Olschewski, A. J., Pullamsetti, S. S., Schermuly, R. T., Stenmark, K. R., & Rabinovitch, M. (2019). Pathology and pathobiology of pulmonary hypertension: State of the art and research perspectives. *The European Respiratory Journal, 53*, 1801887.